South African Journal of Botany 189 (2026) 55–67

Contents lists available at ScienceDirect

South African Journal of Botany

journal homepage: www.elsevier.com/locate/sajb

# DNA barcoding and anti-tyrosinase activities of three species-representative populations of the genus *Greyia* Hook & Harv

Iné Botha [a], Marco N. De Canha [b], Kenneth Oberlander [c], Jana Botes [a], Namrita Lall [b], Dave K. Berger [a,*]

[a] Department of Plant and Soil Sciences, Forestry and Agricultural Biotechnology Institute, University of Pretoria, Pretoria, South Africa
[b] Department of Plant and Soil Sciences, University of Pretoria, Pretoria, South Africa
[c] H.G.W.J. Schweickerdt Herbarium, Department of Plant and Soil Sciences, University of Pretoria, Pretoria, South Africa

ARTICLE INFO

Edited by: Dr. J.S. Boatwright

*Keywords:*
Chalcone
Hyper-pigmentation
ITS
*trnL-F*
*matK*
*psbA-trnH*
Bottlebrush tree
Drakensberg

ABSTRACT

The tree genus *Greyia* is endemic to South Africa and Eswatini. The Eastern Cape species *Greyia flanaganii* Bolus is confined to a limited range west of the Kei River. *Greyia radlkoferi* Szyszyl. occurs in Limpopo Province, whereas *Greyia sutherlandii* Hook. & Harv. is associated with KwaZulu-Natal Province, but the ranges of these two species overlap in Mpumalanga Province. *Greyia* trees are of value to the bioeconomy as leaf extracts from *G. flanaganii* and *G. radlkoferi* possess anti-tyrosinase activity and low toxicity and are being developed in herbal formulations for the treatment of skin hyper-pigmentation. The main active compound is 2',4',6' trihydroxydihydrochalcone. However, there are no reports of medicinal assays from *Greyia* trees growing in their natural habitat, it is not known whether the third species - *G. sutherlandii* - has activity, and DNA barcode data is limited. To address these knowledge gaps, we sampled five trees per *Greyia* species that matched morphological descriptions and were from sites close to type specimen collection records. Leaf ethanolic extracts from *G. sutherlandii* had similar average anti-tyrosinase activity ($IC_{50}$ = 84 μg/mL ± 18 [SD]) when compared to *G. radlkoferi* (58 μg/mL ± 21) and *G. flanaganii* (72 μg/mL ± 11). High Performance Thin Layer Chromatography showed the presence of the active compound in all three species, although it was below the detection limit of 4.4 μg/10 mg extract in two of the *G. flanaganii* samples. Considering the difficulty in differentiating *G. sutherlandii* from *G. radlkoferi* morphologically in the field and production orchards, we investigated DNA barcoding as a method of species-specific authentication. Phylogenetic analysis using Bayesian Inference from combined ITS, *trnL-F, matK* and *psbA-trnH* barcodes from the 15 *Greyia* trees plus Genbank sequences indicated (i) clear differentiation from other lineages in the order Geraniales, but (ii) extremely short internal branches within *Greyia* and poor discrimination between *Greyia* species and individuals. Our study has shown that natural populations of all three species sampled in late summer exhibit consistent leaf anti-tyrosinase activity between biological replicate trees. We have demonstrated activity from *G. sutherlandii* for the first time, indicating that this species can also be deployed in production orchards. However, alternative phylogenetically informative SNP markers need to be developed to provide species-specific authentication of *Greyia* extracts in herbal products.

## 1. Introduction

The genus *Greyia* Hook & Harv is endemic to South Africa and Eswatini. It consists of three species that grow as shrubs or trees, namely *Greyia sutherlandii* Hook. & Harv., *Greyia radlkoferi* Szyszyl., *and Greyia flanaganii* Bolus (Killick and Kimpton, 1977; Phillips and Gower, 1923; Steyn et al., 1999). *Greyia* species are prominent members of grassland biomes in South Africa, with the Eastern Cape species *G. flanaganii* growing at low altitudes mostly along the western tributaries of the Kei River [(Dahlgren and Van Wyk, 1988; Mbambezeli, 2002), Fig. 1A]. Morphologically and phenologically this species is the most distinct, since it has lax bell-shaped hanging flowers, is evergreen, and its distribution is disjunct with the other two species (Fig. 1A, D). On the other hand, both *G. sutherlandii* and *G. radlkoferi* grow in montane grasslands with *G. sutherlandii* centred around the Drakensberg and KwaZulu-Natal, with *G. radlkoferi* the most northerly species in Limpopo [(Dahlgren and

* Corresponding author.
*E-mail address:* dave.berger@fabi.up.ac.za (D.K. Berger).

https://doi.org/10.1016/j.sajb.2025.11.035
Received 19 August 2025; Received in revised form 14 November 2025; Accepted 17 November 2025
Available online 26 November 2025

Van Wyk, 1988), Fig. 1A]. Field guides indicate overlapping distributions in Mpumalanga and Eswatini (Schmidt et al., 2002; Van Wyk and Van Wyk, 2013). The two deciduous species produce striking scarlet inflorescences with copious nectar in late winter/early spring utilized by bird, bee and butterfly pollinators (De la Cruz, 2016; Mbambezeli, 2016). Their floral displays in shades of red stand out against the bare branches prior to leaf set, leading to the common name "beacon tree" (Fig. 1B, C). However, the most widely adopted vernacular name is "bottlebrush tree" on account of the structures of the *G. radlkoferi* and *G. sutherlandii* inflorescences (Fig. 1B, C). The name Woolly Bottlebrush refers to the white woolly appearance of the abaxial surface of *G. radlkoferi* leaves (Fig. 1B). In contrast, the Natal Bottlebrush

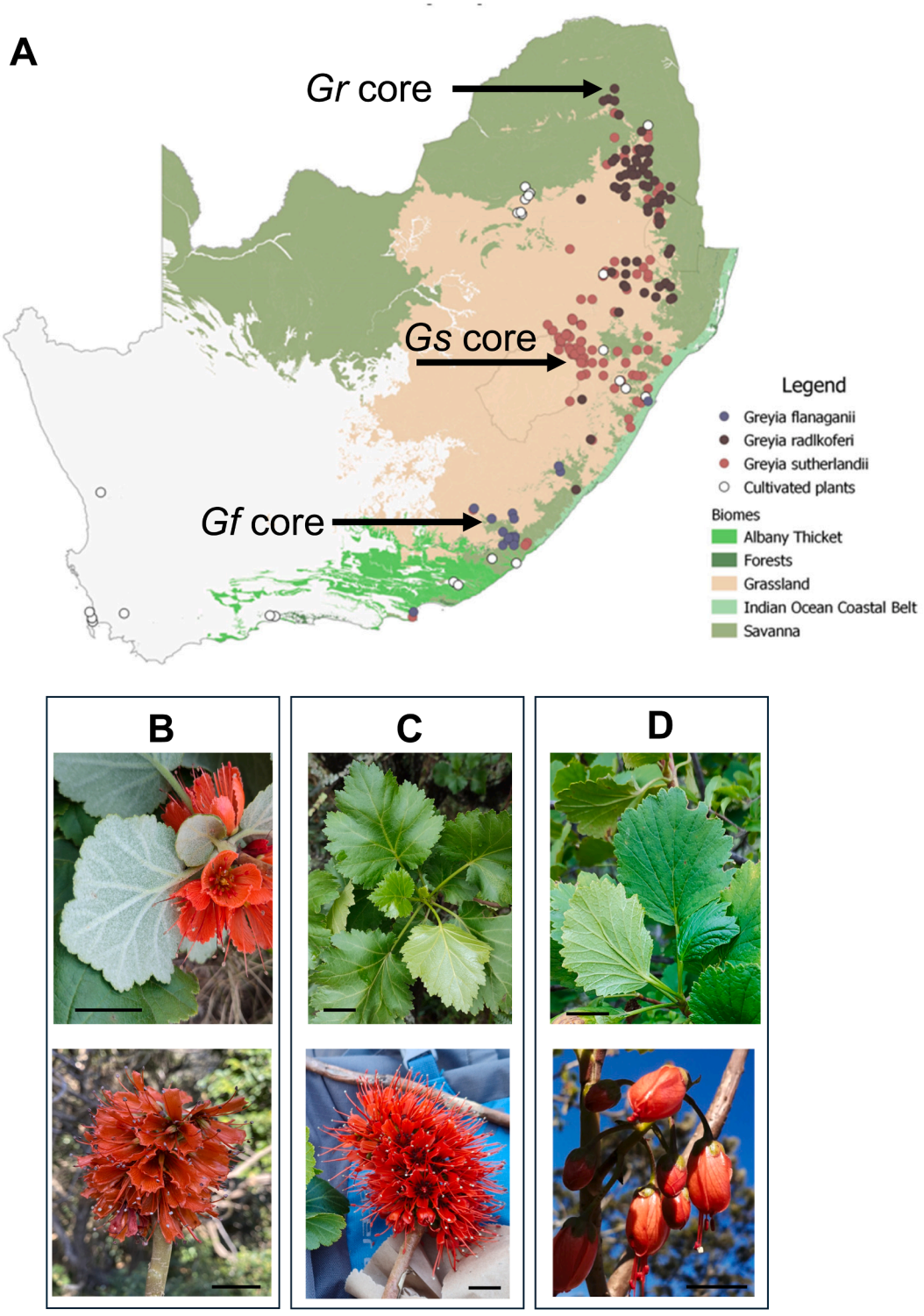


**Fig. 1.** *Greyia* herbarium specimen distributions and morphology. A: Biome map of South Africa with distribution of PRE and PRU herbarium records labelled as *Greyia radlkoferi* (brown dots), *Greyia sutherlandii* (red), *Greyia flanaganii* (blue), or cultivated (white). The sampling sites of the "core population" of each species are marked with arrows. Map drawn in 2021 using QGIS software. B – D: Representative leaf and inflorescence morphologies of sampled core populations of *G.radlkoferi, G.sutherlandii*, and *G.flanaganii*, respectively. Photos: DK Berger. Scale bars = 2 cm.

(*G. sutherlandii*) and the Kei Bottlebrush (*G. flanaganii*) generally have glabrous leaves (Fig. 1C, D). Currently there is minimal DNA information for the genus *Greyia* with only a handful of DNA sequences in public databases (Linder et al., 2006; Palazzesi et al., 2012).

Prior to DNA-based systematics, taxonomic classification of the genus *Greyia* Hook. & Harv. based on morphology was conducted in the late 1800's, which recognised *G. sutherlandii* Hook. & Harv. (Harvey, 1859), *G. radlkoferi* Szyszyl. (Szyszyłowicz, 1888), and *G. flanaganii* Bolus (Hooker, 1895). *Greyia* has been difficult to place taxonomically, with different authors placing it in either Saxifragaceae, Melianthaceae or a new family Greyiaceae (Dahlgren and Van Wyk, 1988). More recent, mostly molecular-based classifications have convincingly placed *Greyia* in the Order Geraniales (The Angiosperm Phylogeny Group [APG] I, II, III, IV). However, the familial placement of *Greyia* remains controversial. According to APGIII, *Greyia* was placed in a broadly interpreted Melianthaceae, however in APGIV narrower family-level circumscriptions resulted in assignment to Francoaceae due to nomenclatural precedence (The Angiosperm Phylogeny Group, 2016). Members of the Geraniales *sensu* APGIV have a diverse geographical distribution with some families endemic to South America or Africa. Palazzesi et al. (2012) show DNA data phylogenies (ITS, *trnL-F*) for more members of the Geraniales than Linder et al. (2006) and reported the familial classification adopted by APGIV as follows: (i) Melianthaceae: *Melianthus* spp. (South Africa) group with *Bersama* spp. (Africa), separate from (ii) Francoaceae made up of *Francoa* spp. (Chile) which group with *Greyia* spp. (South Africa), and separate from (iii) Vivianaceae: *Viviana* spp. (Chile, Brazil), *Balbisia* spp. (Argentina, Chile, Brazil), *Rhynchotheca* sp. (Andes). These are separate from a clade that includes Geraniaceae (worldwide) and Hypseocharitaceae (Argentina, Peru) (The Angiosperm Phylogeny Group, 2016). Sytsma et al. (2014) followed up from Palazzesi et al. (2012) suggesting some corrections to the chronogram and timing of divergence between clades. Their chronogram supported the conclusion that species within *Melianthus* and *Bersama* diversified due to the aridification over Southern Africa in the past 5 million years. Linder et al. (2006) also proposed aridification in the region as driving diversification. Due to the small number of polymorphisms in barcode data available, the *Greyia* spp. are thought to have diversified more recently (3.2 Mya or less). Jeiter et al. (2017) studied the flower morphology of Geraniales, and their results mostly supported the phylogeny of Palazzesi et al. (2012). This corroborated earlier morphological work in which floral character states grouped *Greyia* with other genera in the Francoaceae (Ronse Decraene and Smets, 1999).

DNA barcoding is a molecular identification method that is based on sequencing of short standardized DNA regions (Kress, 2017). DNA barcoding has many applications, with a primary role as a tool to quantify biodiversity for conservation planning (Krishna Krishnamurthy and Francis, 2012; Rattray et al., 2024). The International Barcode of Life Consortium is an effort to centralize and standardize global biodiversity information based on DNA barcodes (Ratnasingham et al., 2024). It provides a valuable resource for research but also stimulates citizen science. A local example is the Foundational Biodiversity Information Programme in South Africa (Rattray et al., 2024). DNA barcoding is utilized in forensic applications for tracing the trafficking of endangered plant species, monitoring invasive taxa, detecting plant material in dietary studies or cases of food adulteration, monitoring allergenic pollen (Whitley et al., 2024), diagnosing plant diseases (Meisel et al., 2009), and verifying the authenticity of herbal products (Raclariu et al., 2018).

In order to be considered as a good barcode, the DNA marker should be sufficiently divergent between species (but not within species); have conserved flanking regions for universal primers; be short enough for easy PCR amplification; and have a high taxonomic coverage and resolution (Kress and Erickson, 2008). In plants, the nuclear ITS region and several plastid gene regions (e.g. *rbcL, matK, trnL-F, psbA-trnH*) have proven to be the most effective DNA barcodes (Kress, 2017). In the search for a "universal" plant barcode, some authors have recommended gene combinations such as *matK/rbcL* (CBOL-Plant-Working-Group, 2009), or the ITS2/*psbA-trnH* combination (Chen et al., 2010). However, development of universal primers for all plants has been elusive. Therefore, empirical research on a taxon-specific basis is required to develop DNA barcodes that are effective to a species level, especially for recently diverged taxa.

DNA barcode data for the genus *Greyia* is limited. In a study focused on the genus *Melianthus* (Linder et al 2006), DNA barcodes were generated for *G. radlkoferi* and *G. flanaganii* to use as outgroups in the phylogenetic analysis, which confirmed the monophyly of *Melianthus* distinct from *Greyia*. These authors reported ITS, *trnL-F* and *psbA-trnH* sequences for one *G. radlkoferi* and one *G. flanaganii* individual in cultivation but the natural provenance of these trees is unknown (Linder et al 2006). The only other DNA barcode data on Genbank are ITS and *trnL-F* for one individual each of *G. radlkoferi, G. flanaganii* and *G. sutherlandii* derived from herbarium specimens in Germany, also with no provenance data (Palazzesi et al, 2012). These DNA barcodes have only one or two polymorphisms between the *Greyia* spp. with inconsistencies between individuals of the same species. It is not known if these are intra-specific differences or sequencing errors (Linder et al., 2006; Palazzesi et al., 2012).

The genus *Greyia* is not only important for its conservation value in natural areas along the Great Escarpment of southern Africa, but also for its medicinal properties. This is because extracts from *Greyia* spp. leaves have potential to be used as a treatment of skin hyper-pigmentation (De Canha and Lall 2019). Hyper-pigmentation occurs in skin patches where there is over-production of tyrosinase, resulting in excess melanin production. Chemical agents such as kojic acid with anti-tyrosinase activity are often used to treat the condition, but they may have negative side effects (De Canha and Lall 2019), which necessitates the development of alternative treatments. Herbal remedies from African flora serve as prominent candidates, with extracts from a range of South African plants, such as *Combretum collinum* Fresen, *Schotia brachypetala* Sond, and *Vachellia nilotica* (L.) P.J.H. Hurter & Mabb, exhibiting anti-tyrosinase activity (Lall, 2019).

Previous studies reported that ethanolic leaf extracts of cultivated *G. radlkoferi* and *G. flanaganii* trees had significant anti-tyrosinase activity without negative cytotoxic or mutagenic effects (Mapunya et al. 2011; Lall et al. 2016). The active biomarker compound was identified as 2',4',6' trihydroxydihydrochalcone with $IC_{50}$ values of 17.70-17.86 μg/ml (Lall et al. 2016). A second compound from the extracts, 3,5,7-trihydroxyflavone (galangin), had minor additional activity ($IC_{50} = 113.60$ μg/ml; Lall et al. 2016).

*Greyia* production orchards have been planted in Gauteng, South Africa, supported by ongoing horticultural research (Malele et al., 2021). These initiatives will play an important role in limiting over-harvesting from wild populations of *Greyia*. However, planting material was sourced from local nurseries, and species identities and provenances are therefore unknown. Screening of the orchard plants shows high variability in leaf morphology (woolly vs glabrous) and anti-tyrosinase activity (Ing et al., 2020). Previous authors have also highlighted the unreliability of leaf morphology in differentiating *G. radlkoferi* from *G. sutherlandii*, especially in the field where species ranges overlap (Dahlgren and Van Wyk, 1988; Steyn, 1974). Currently, data on *Greyia* anti-tyrosinase activity is limited to a few cultivated individuals of *G. radlkoferi* and *G. flanaganii*, and no species-verified *G. sutherlandii* have been assayed.

Therefore, there is a gap in knowledge about the medicinal activity of wild populations of the three *Greyia* species, especially *G. sutherlandii*, and a need to establish a reliable species diagnostic assay, possibly with DNA barcoding. Considering the dearth of DNA data for the genus *Greyia*, there is also a need to collect DNA barcode data to support the Foundational Biodiversity Programme in South Africa. Furthermore, the SANBI Biosystematics research strategy has prioritized the *Greyia* genus for taxonomic revision (SANBI, 2024).

## 2. Materials and methods

### 2.1. Greyia plant selection

Distribution data of *Greyia* specimens was obtained from National Herbarium Collections [SANBI PRECIS database, GBIF (https://www.gbif.org/)], the Pretoria National Herbarium (PRE), and the H.G.W.J. Schweickerdt Herbarium (PRU) at the University of Pretoria. A distribution map was drawn using *QGIS Desktop v3.34.2* using the SANBI vegetation map as a base layer shape file (https://www.sanbi.org/biodiversity/foundations/national-vegetation-map/). The JSTOR Global Plants Database (https://plants.jstor.org/) was used to search for herbarium records of type specimens of *Greyia* spp. The resulting type specimen data was used to verify that a selected core population of each species was located near putative collection sites for type specimens of each species. For *G. sutherlandii* Hook. & Harv. the type specimen in Harvey (1859)(# TCD0001762 at the Trinity College Herbarium, Dublin, with a replicate #PRE0588133) has a collection site of "near Port Natal", which is now Durban. In addition, specimens #MEL 0250775A and MEL 0250776A which are listed as "Type" at the National Herbarium of Victoria, Melbourne, Australia) collected by PC Sutherland have the location "Klip River". The replicate "Klip River" specimen at Royal Botanical Gardens Kew #K000310099 has an annotation slip "Collected in the Quathlamba or Drakensberg", mostly likely written by PC Sutherland in his notoriously illegible handwriting. For *G. radlkoferi* Szyszyl., named in Szyszyłowicz (1888) the type specimen #6404 (Accession Z-000018561 at the Zurich Herbarium) was collected by A. Rehmann at Houtbosh, which is likely the current Woodbush Forest Reserve, Limpopo Province. For *G. flanaganii* Bolus in Hooker (1895), the type specimen #328 (Accession BOL121746 at the Bolus Herbarium) has a collection site of "near Komgha", however a subsequent georeferencing project placed the site at QDS = 3227DB (near Stutterheim), Eastern Cape Province.

### 2.2. Greyia plant material sampling

At each core population, ten to fifteen mature leaves per *Greyia* tree, from five individuals, were sampled at the same time of year (January-March) and kept on ice for phytochemical extractions. Young leaf material (newly emerged flush) from each *Greyia* tree was sampled into ziplock bags containing silica gel bead desiccant (Merck, catalogue # 1077351) and stored at room temp until gDNA extraction. Herbarium specimens of reproductive and vegetative material from representative trees of each species' core population were sampled and deposited at the H.G.W.J. Schweickerdt Herbarium (PRU) at the University of Pretoria. *Greyia* sampling was conducted with research permits issued by the Limpopo Economic Development, Environment and Tourism, Ezemvelo KZN Wildlife, and the Eastern Cape Economic Development, Environment Affairs and Tourism.

### 2.3. Greyia leaf ethanolic extractions

Approximately 30 g of fresh *Greyia* leaf material was ground in liquid nitrogen using a mortar and pestle until a fine powder was formed. An extract was made from the ground material with 98 % ethanol (EtOH 98 %) in a 1:10 (w/v) ratio. The extracts were placed on an orbital shaker at 135 rpm for 72h (Labotec, Midrand, South-Africa), and subsequently filtered using a vacuum filtration system with a Buchner funnel fitted with a Whatman 1.0 filter paper (Sigma Chemical Co., St. Louis, USA). The filtered extracts were concentrated using a Rotary Evaporator (Buchi Rotavapor R-114, Labotec, Midrand, South-Africa). A fume hood was used to air dry the extracts for one to two weeks.

### 2.4. Tyrosinase inhibition assay

The tyrosinase inhibition assay was performed according to the methods described by (Lall et al., 2016; Mapunya et al., 2011) with modifications. The *Greyia* leaf extracts were solubilized to a stock concentration of 10,000 μg/mL in 100 % DMSO in an Eppendorf tube. In a 96-well plate (sample preparation plate), 200 μL of the extract stock concentration was added to the first row and 100 μL of 100 % DMSO was added to seven subsequent wells. The extracts were then serially diluted two-fold to obtain eight final concentrations ranging from 78.125 – 10,000 μg/mL. For kojic acid (Merck Pty. Ltd, South Africa; Batch: 1363411V), the positive control, a stock concentration of 1000 μg/mL (in DMSO) was prepared and diluted similarly to the extracts to obtain eight concentrations ranging from 7.8125 - 1000 μg/mL. Thereafter, in a separate 96-well plate (test plate), 100 μL of 50 mM potassium phosphate buffer (pH 6.5), 10 μL of sample dilutions (from the sample prep plate) and 10 μL of mushroom tyrosinase enzyme (1000 U/mL) (Merck Pty. Ltd, South Africa; Batch: SLBM7158V) were added and incubated at 37°C for 10 minutes, followed by the addition of 80 μL of L-tyrosine substrate (2.65 mM) (Merck Pty. Ltd, South Africa; Batch: BCBZ5546). Final concentrations of the extracts ranged from 3.91 - 500 μg/mL while for kojic acid final concentrations ranged from 0.196 μg/mL - 50 μg/mL. Immediately after addition of the substrate, a kinetic read (70 reads, 14 s intervals) was performed at an optical density of 492 nm using a BIO-TEK PowerWave XS multi-well plate reader (Analytical and Diagnostic Products, Weltevreden Park, South Africa). For data analysis, the samples were compared to the controls which consisted of a 5 % v/v DMSO vehicle control (100 % enzyme activity) and 0 % activity (tyrosinase enzyme with no substrate). GraphPad Prism 4.0 software was then used to calculate the $IC_{50}$ value for each reaction as follows: the concentrations (X-values) were transformed using X = LogX function, followed by normalisation of the data to the 0 % and 100 % enzyme activity (constraints set to 0 and 100) and finally a non-linear regression (curve fit) was carried out using a sigmoidal dose-response (variable slope). Goodness of fit values are shown in Table S1.

### 2.5. Statistical analysis

Statistical analysis of the *Greyia* extract anti-tyrosinase activities ($IC_{50}$ values, calculated as described in section 2.4) was carried out in the R statistical environment (R Core Team, 2024). Extracts from five biological replicate trees each of *G. flanaganii* and *G. radlkoferi*, and four biological replicate trees of *G. sutherlandii* (P245 material was not available at the time of sampling) were assayed for inhibition of tyrosinase activity in three independent technical replicate trials. The averages of the technical replicates per tree were used for statistical analysis. To determine whether there was a significant "*Greyia* species" effect on tyrosinase activity, the ggtukey package in R was used to perform Tukey's Multiple Comparison Test with a 5 % threshold for significance (Bass, 2022), and the data was visualized with a boxplot drawn using the ggplot2 R package (Wickham, 2016).

### 2.6. High performance thin layer chromatography and biomarker quantification

#### 2.6.1. Preparation of reference compounds and Greyia extracts

For phytochemical profiling, 10 mg of each *Greyia* leaf ethanolic extract was weighed in a 2.0 mL Eppendorf tube, followed by the addition of 1000 μL of absolute ethanol (EtOH). The samples were then vortexed for 20 seconds before being placed in an ultrasonic bath for 15 mins at 30°C. Similarly, the two reference compounds, 2′,4′,6′-trihydroxydihydrochalcone and 3,5,7-trihydroxyflavone (galangin) (Merck, South Africa) were prepared to a stock concentration of 2 mg/mL (in

EtOH). The reference compounds were mixed 1:1 (500 μL: 500 μL) and subsequently serially diluted two-fold in EtOH, to a concentration range of 31.25, 62.50, 125, 250 and 500 μg/mL. All samples and standards were then placed on a Spectrafuge Mini C1301 (Labnet International, Inc.) at 6000 rpm (2000 g) for 30 seconds to remove any sediment (undissolved solid particles) before 500 μL was transferred to a 2 mL HPTLC crimp vial. The vials were then placed in their respective position in the sample tray of the Automatic TLC Sampler 4 (ATS4) (CAMAG, Switzerland) for HPTLC analysis.

#### 2.6.2. Reference compound and sample application

Glass-backed HPTLC plates (20 × 10 cm, silica gel 60 $F_{254\ nm}$) were visualised using the TLC Visualiser 2 (CAMAG, Switzerland) to obtain a clean plate image. The standards and extracts were applied to the plate using the ATS4 (CAMAG, Switzerland). Reference compounds and extracts were applied as 8 mm bands with a separation distance of 11.4 mm and 20 mm from the left edge. For each concentration of the reference compound mixture, 10 μL was applied and for each *Greyia* leaf extract, 20 μL was applied. The limits of detection for each reference compound were 0.3125 – 5.00 μg per spot.

#### 2.6.3. HPTLC plate development

Following sample application and acquisition of the clean plate images using the TLC Visualiser 2 (CAMAG, Switzerland), HPTLC plates were developed to a migration distance of 70 mm using the Automatic Developing Chamber 2 (ADC2) (CAMAG, Switzerland), with a mobile phase consisting of toluene, ethyl acetate and formic acid (7:3:0.1 v/v/v), then saturation for 20 min (with a saturation pad) and finally activation ($MgCl_2.6H_2O$ for 10 min). After development, plates were dried for 5 minutes in the ADC2 (CAMAG, Switzerland). The dried, developed HPTLC plates were then visualised prior to derivatization under white light (remission [R], remission-transmission [RT] and transmission [T]), 254 nm and 366 nm using the TLC Visualiser 2 (CAMAG, Switzerland).

#### 2.6.4. Post-chromatographic derivatization with NP reagent and p-anisaldehyde

Developed plates were heated to 100°C for 3 mins using the TLC Plate Heater 3 (CAMAG, Switzerland) and allowed to cool for 5 mins before derivatization with 200 mL of natural product (NP) reagent (2 g of 2-aminoethyl diphenyl borinate in 200 mL of ethyl acetate) using the Immersion Device 3 (CAMAG, Switzerland) (Dipping Speed: 5; Dipping Time: 0). Thereafter, the plates were air-dried for 5 mins before capturing images using the TLC Visualizer 2 (CAMAG, Switzerland) at R, RT, T and 366 nm. A second derivatization step was then performed using 200 mL of *p*-anisaldehyde (170 mL of ice cold MeOH, 20 mL acetic acid, 10 mL $H_2SO_4$ and 1 mL of *p-anisaldehyde*) in the Immersion Device 3 (CAMAG, Switzerland) (Dipping Speed: 5; Dipping Time: 0). Plates were then allowed to air dry for 5 mins followed by heating at 100°C for 3 mins using the TLC Plate Heater 3 (CAMAG, Switzerland). The derivatized plates were then cooled to room temperature before capturing images under R, RT, T and 366 nm using the TLC Visualizer 2 (CAMAG, Switzerland).

#### 2.6.5. Quantification of reference standards in sample tracks

For the densitometric quantification of the reference compounds, image profiles were generated using VisionCATS 4.0 software. Quantification of 2',4',6'-trihydroxydihydrochalcone was performed using profiles generated from *p*-anisaldehyde derivatized plate images, illuminated under RT=Remission-Transmission (light from the top and bottom of the plates), where the 2′,4′,6′-trihydroxydihydrochalcone appeared as an orange band with $R_f = 0.34$. For quantification of 3,5,7-trihydroxyflavone (galangin), image profiles generated from developed plates under UV 254 nm without derivatization were used. The compound appeared as a black band at $R_f = 0.53$. For quantification of the reference compounds from the standard curves, a deviation range of 5.00 % was used, any samples falling outside of the standard curve regression more than 5.00 % were excluded from the quantification and reported as "excluded from regression". Extracts containing quantities of the two reference compounds which were within the calibration curve concentration range (expressed as μg/ 20 μL) were then used to calculate the concentration in 1 000 μL, which equated to the concentration in 10 mg of extract (dissolved in 1 000 μL). Sample tracks with no reference compound assignment were recorded as "not detected (nd)".

### 2.7. Greyia genomic DNA extraction

Pilot DNA extractions indicated high amounts of secondary metabolites in *Greyia* leaves which co-purified with genomic DNA (gDNA) and inhibited PCR reactions (data not shown). To mitigate this the gDNA was extracted based on the CTAB method used by (Stewart and Via, 1993) with modifications that included adding polyvinyl pyrrolidone (PVP) (Michiels et al., 2003) and sodium sulfite (Byrne et al., 2001), as well as a high concentration of β-mercaptoethanol (BME) to prevent oxidation of these secondary metabolites. The CTAB buffer was first activated by adding BME and polyvinyl pyrrolidone (PVP-10). Briefly, approximately 100-200 mg plant material was ground with a mortar and pestle in the presence of liquid nitrogen. The ground plant material was transferred to a 2mL Eppendorf tube and 800 μL of 65°C pre-warmed activated CTAB extraction buffer (2 % w/v CTAB; 100mM Tris-Cl, pH8; 20mM EDTA, pH8, 1.4M NaCl, 80mM sodium sulfite with 5 % w/v PVP10 powder and 2 % v/v BME) was gently added. It was vortexed and placed in a water bath at 65°C for 60 minutes, and occasionally mixed by inversion. An equal volume of chloroform: isoamyl alcohol (24:1) was added. The mixture was centrifuged for 15 minutes (20 800 rcf). The supernatant was collected, and DNase free RNase A (1 μg/mL final concentration) was added and incubated at 37°C for 30 minutes. Phenol: Chloroform: isoamyl alcohol (25:24:1) was added, the solution was vortexed and centrifuged as before. The aqueous phase was collected and an equal volume of propan-2-ol was added and the solution was left at -20°C for 1 hour to allow for DNA precipitation. The solution was centrifuged as before, the DNA pellet was washed twice with 500 μl of 70 % EtOH and resuspended in 70 μl $ddH_2O$ or TE buffer (10 mM Tris, 1mM EDTA, pH 7.5).

### 2.8. PCR amplification of DNA barcoding genes

PCR amplification was done based on Linder et al. (2006) with slight adjustments. The following oligonucleotide primers were used: *ITS*4 and *ITS*5 (Baldwin et al., 1995), and *trnL-F* (c and f) or (e and f) primers (Taberlet et al., 1991). The *psbA* primer was as described in (Sang et al., 1997), but a custom-designed trnH(*Greyia*) primer was used 5'-CGCGCATGGTGGATTCACAATCC-3'. In addition, internal *matK* primers which flanked an informative SNP were designed and deployed (*matK*-F161: 5′-CGGTCCTTTCTCCACGAATA-3′; *matK*-R619 5′-GTCGAGGGAATGCTTGGATA-3′). Primers were synthesized by Inqaba Biotechnical Industries (Pty) Ltd, Pretoria, South Africa. The PCR conditions were set up as follows: 5 min at 94°C, 5 cycles of 1 min at 94°C, 2 min at 55°C for ITS (52°C for *trnL-F*) and 2 min at 72°C, then the PCR conditions are changed to 1 min at 94°C, 30s at 55°C, 45s at 72°C for 30 cycles and then a final elongation for 5 min at 72°C. For *matK* and *psbA-trnH* the PCR conditions were 3 min at 96°C, 30s at 59°C, 45s at 72 C for 35 cycles and then a final elongation for 5 min at 72°C. Each PCR reaction (10 μL) contained 3X Taq DNA polymerase Master Mix (#A180306, Amplicon, Lasec, Ndabeni, Cape town) (3 μl), 3 mM MgCl, 5 % DMSO (Sigma), 0.5 μM forward primer, 0.5 μM reverse primer, and 1 μL gDNA (maximum concentration 1 ng/μL).

### 2.9. Sanger sequencing of DNA barcoding genes

PCR products were purified by agarose gel electrophoresis followed by the Zymoclean™ gel extraction kit (Inqaba Biotec). Alternatively, 3ul of ExoSAP-IT reagent (ThermoFischer) was added to each 10 uL PCR

reaction, incubated at 37°C for 15 min, followed by 80°C for 15 min. Sanger sequencing reactions were conducted with the BigDye v3.1 (Life Technologies, Johannesburg, South Africa) reagent, followed by an Ethanol precipitation. DNA sequencing was conducted on an ABI 3500xl Genetic Analyzer at the DNA Sanger Sequencing Facility at the University of Pretoria. DNA sequence analysis and preliminary alignments were carried out using QIAGEN CLC Main Workbench (QIAGEN, Aarhus, Denmark) or Geneious Prime 2025.1.2 (https://www.geneious.com). *Greyia* ITS, *matK, trnL-F* and *psbA-trnH* barcode sequences have been deposited at www.boldsystems.org and GenBank (see Fig. 4 legend for details).

### 2.10. Phylogenetic analysis

To provide context on DNA sequence variation in standard barcode regions in *Greyia*, sequenced accessions for all four markers were compared to other members of the order Geraniales, using *Geranium incanum* Burm. f. and *Pelargonium incrassatum* (Andrews) Sims as outgroup representatives of the Geraniaceae. Sampling initially followed Linder et al. (2006), supplemented by more recent accessions of each barcode marker available on GenBank (https://www.ncbi.nlm.nih.gov/). Accession information is provided in the relevant figures. Each individual marker was aligned using the ClustalW functionality embedded in BioEdit v7.2.3 (Hall, 1999), with subsequent manual alignment. The amino acid translation of *matK* was used to improve alignment of this marker. The *psbA-trnH* alignment proved very difficult to align across the order due to many large indels and a high AT bias; the canonical *psbA-trnH* RNA loop (Štorchová and Olson, 2007) was also difficult to align due to multiple inversions across Geraniales, and was excluded from analysis.

Aligned markers were analysed using Bayesian inference in MrBayes v3.2 (Ronquist et al., 2012). All analyses used reversible jump Markov Chain Monte Carlo (rjMCMC) to average over model space as well as tree space, with an included gamma correction factor to account for among-site rate variation. All analyses were run for a total of 5 million generations, sampling every 5000 generations, using the default two independent runs implemented in MrBayes. The *matK* alignment was partitioned according to codon position as this significantly improved model fit in preliminary runs; each position had its own model of nucleotide substitution inferred using rjMCMC and a separate gamma factor. A combined analysis featuring all four markers was also run, partitioned according to marker, with each partition assigned its own model as for the individual marker analyses. Outside of *Greyia*, all species from the individual analyses that had at least two markers available were included in the combined analysis. All other settings were as for the individual marker analyses. All runs were judged for sample size and convergence on the posterior using MrBayes's own diagnostics, as well as visually in Tracer v1.7.3 (Rambaut et al., 2018).

To assess the barcoding gap, intra-specific vs interspecific pairwise distances for the three *Greyia* species were estimated and assessed using the function threshID() in the package 'spider' (Brown et al, 2012) (Brown et al., 2012) in the R statistical environment (R Core Team, 2024), under the K2P substitution model and default threshold of 0.01.

## 3. Results

### 3.1. Distribution map and sample selection

To achieve the goals of this study, it was important to identify wild-growing *Greyia* trees with the highest likelihood of representing each of the three described species *G. radlkoferi, G. sutherlandii* and *G. flanaganii*. Our strategy was (i) to map the locations of *Greyia* herbarium specimens at PRE and PRU; (ii) select locations with single species identities that were geographically distant from other species, and that were accessible for research sampling, (iii) verify whether these locations corresponded to the provenances of type specimens, and (iv) sample five trees at each species location.

Figure 1A shows the geographical distribution of *Greyia* samples at PRE and PRU. Generally, *G. radlkoferi* is distributed in Limpopo and Mpumalanga Provinces, with *G. sutherlandii* in Mpumalanga and KwaZulu-Natal (Drakensberg), and *G. flanaganii* in the Eastern Cape (Fig. 1A). Therefore, we sampled five *G. radlkoferi* trees (named P001-P005) near Modjadjiskloof, Limpopo Province at a site 9 km from Woodbush Forest Reserve (collection site of type specimen); five *G. sutherlandii* trees at Monks Cowl Nature Reserve (P241-P245), Central Drakensberg, KwaZulu-Natal; and five *G. flanaganii* trees (P157-P161) at Nyara river, a tributary of the Kei River, Eastern Cape which is in the same Quarter Degree Square (QDS) location as the type specimen (Table 1, Fig. 1A). We termed these "core populations" for the purposes of the study.

### 3.2. Morphological traits

At sampling we verified that trees from each core population exhibited similar field morphology that matched each species description (Killick and Kimpton, 1977; Phillips and Gower, 1923; Steyn et al., 1999). Representative images of each species core population are provided in Figure S1, which shows sampled trees in their natural habitat, inflorescence morphology, and leaf morphology (adaxial and abaxial). The five trees from the core *G. radlkoferi* population had woolly leaves, especially on the abaxial side, and compact racemes with many red flowers, illustrated in Fig. 1B (Table 1). All five *G. sutherlandii* and five *G. flanaganii* trees had shiny glabrous leaves (Fig. 1C, 1D, Table 1). The *G. flanaganii* core population trees had the distinct lax pendulous bell-shaped red flowers (<12) (Fig. 1D), whereas the *G. sutherlandii* trees had racemes with many red flowers similar to *G. radlkoferi*, and were more elongated although differentiation using this trait was not clear (Fig. 1B, 1C, Table 1).

### 3.3. Anti-tyrosinase activity and biomarker quantification of leaf extracts from wild-growing Greyia

The previously described medicinal activity of *Greyia* was based on the anti-tyrosinase activity of leaf extracts attributed to flavonoid compounds of single *G. flanaganii* and *G. radlkoferi* trees grown in cultivation (Lall et al., 2016; Mapunya et al., 2011). This study aimed to evaluate the activity of wild-growing trees of all three species, since a species-verified *G. sutherlandii* had not previously been tested. Ethanolic leaf extracts from the five core trees of each species sampled at the same time of year (late summer) were prepared according to established protocols and assayed for inhibition of tyrosinase enzyme activity (Lall et al., 2016).

Representative images of the leaves of each *Greyia* species core population used for the ethanolic extractions are shown in Figure S1. *G. sutherlandii* extracts exhibited average $IC_{50}$ values (84 ± 18 μg/mL) that were not significantly different from the extracts from *G. radlkoferi* (58 ± 21 μg/mL) and *G. flanaganii* (72 ± 11 μg/mL)(Tukey's Multiple Comparison Test, alpha = 0.05)(Fig. 2). The positive control kojic acid had high tyrosinase inhibition ($IC_{50}$ = 4.5 ± 1.3 μg/mL).

High Performance Thin Layer Chromotography was carried out to determine the presence of the active compounds in the *Greyia* ethanolic leaf extracts. This was performed by including a dilution series (standard curve) of the active compounds 2',4',6'-trihydroxydihydrochalcone and 3,5,7-trihydroxyflavone (galagin) as references on the HPTLC plates. Visualization was conducted using different wavelengths of light after development and after derivatization. The most effective method to quantify 2′,4′,6′-trihydroxydihydrochalcone was after derivatization with natural product (NP) and *p*-anisaldehyde reagents followed by visualization under Remission-Transmission white (visible) light. This compound appeared as an orange band at $R_f$ = 0.34 (Tracks 1-5 (left) in Fig. 3 A, B and C). For all HPTLC images the first five tracks (1-5, left) correspond to the reference compounds 2',4',6'-

**Table 1**
*Greyia* trees sampled in this study.

| Species | Tree code | Herbarium voucher | Location | Province | QDS* | Leaf morphology | Inflorescence morphology | 2,4,6-trihydroxydihydrochalcone (ug/10mg leaf extract)** | 3,5,7-trihydroxyflavone (ug/10mg leaf extract)*** |
|---|---|---|---|---|---|---|---|---|---|
| *G. radlkoferi* | P001 | PRU0130853 | Near Modjajiskloof | Limpopo | 2330CC | Woolly | compact racemes, many flowered | 19.69 | 39.13 |
| *G. radlkoferi* | P002 | PRU0130854 | Near Modjajiskloof | Limpopo | 2330CC | Woolly | compact racemes, many flowered | 8.22 | 34.94 |
| *G. radlkoferi* | P003 | PRU0130855 | Near Modjajiskloof | Limpopo | 2330CC | Woolly | compact racemes, many flowered | 6.13 | 28.48 |
| *G. radlkoferi* | P004 | PRU0130856 | Near Modjajiskloof | Limpopo | 2330CC | Woolly | compact racemes, many flowered | 7.86 | 34.67 |
| *G. radlkoferi* | P005 | PRU0130857 | Near Modjajiskloof | Limpopo | 2330CC | Woolly | compact racemes, many flowered | 16.32 | 43.69 |
| *G.sutherlandii* | P241 | nd | Monks Cowl Nature Reserve | KwaZulu-Natal | 2929AB | Glabrous | elongated racemes, many flowered | 11.77 | 16.92 |
| *G. sutherlandii* | P242 | PRU0133571 | Monks Cowl Nature Reserve | KwaZulu-Natal | 2929AB | Glabrous | elongated racemes, many flowered | 14.73 | 23.72 |
| *G. sutherlandii* | P243 | PRU0133572 | Monks Cowl Nature Reserve | KwaZulu-Natal | 2929AB | Glabrous | elongated racemes, many flowered | 17.41 | 16.74 |
| *G. sutherlandii* | P244 | PRU0133573 | Monks Cowl Nature Reserve | KwaZulu-Natal | 2929AB | Glabrous | elongated racemes, many flowered | 30.28 | 25.72 |
| *G. sutherlandii* | P245 | PRU0132900 | Monks Cowl Nature Reserve | KwaZulu-Natal | 2929AB | Glabrous | elongated racemes, many flowered | nt | nt |
| *G. flanaganii* | P157 | PRU0130828 | Nyara river | Eastern Cape | 3227AD | Glabrous | lax pendulous bell-shaped flowers (<12) | 11.59 | 58.10 |
| *G. flanaganii* | P158 | PRU0129525 | Nyara river | Eastern Cape | 3227BC | Glabrous | lax pendulous bell-shaped flowers (<12) | nd | 44.79 |
| *G. flanaganii* | P159 | PRU0129526 | Nyara river | Eastern Cape | 3227BC | Glabrous | lax pendulous bell-shaped flowers (<12) | 4.38 | 42.40 |
| *G. flanaganii* | P160 | PRU0129527 | Nyara river | Eastern Cape | 3227BC | Glabrous | lax pendulous bell-shaped flowers (<12) | nd | 38.67 |
| *G. flanaganii* | P161 | PRU0129528 | Nyara river | Eastern Cape | 3227BC | Glabrous | lax pendulous bell-shaped flowers (<12) | 9.21 | 73.16 |

*Quarter degree square location
**HPTLC quantification based on derivitization with natural product and p-anisaldehyde reagents visualized with Remission-Transmission light. nd=not detected, nt=not tested.
***HPTLC quantification based on visualization at 254 nm. nd=not detected, nt=not tested.

trihydroxydihydrochalcone and 3,5,7-trihydroxyflavone (galangin), while the subsequent five tracks (1-5, right) correspond to the *Greyia* extracts. For *G. sutherlandii* there were only four extract tracks due to the unavailability of P245 material.

All five *G. radlkoferi* leaf extracts (P001 – P005) had detectable quantities of 2',4',6'-trihydroxydihydrochalcone at $R_f = 0.34$, ranging from 6.13 – 19.69 μg/ 10 mg extract (Fig. 3A, tracks 1-5, right) (Table 1), which was quantified using the biomarker compound standard curve. Three of the *G. flanaganii* ethanolic leaf extracts (P157, P159 and P161), contained the 2′,4′,6′-trihydroxydihydrochalcone (4.38 - 11.59 μg/10 mg extract), visible as the orange band at $R_f \sim 0.34$ (Fig. 3B, tracks 1, 3 and 5, right) (Table 1). All four of the *G. sutherlandii* ethanolic leaf extracts (P241 – P244) had detectable quantities of the 2′,4′,6′-trihydroxydihydrochalcone at Rf = 0.34, ranging from 11.77 – 30.28 μg/ 10 mg extract (Fig. 3C, tracks 1-4, right) (Table 1).

The presence of 2′,4′,6′-trihydroxydihydrochalcone was supported by the peak profiles generated from the NP and *p*-anisaldehyde derivatized plates illuminated under RT light (Fig. S2). The profiles showed peaks of 2′,4′,6′-trihydroxydihydrochalcone at $R_f \sim 0.34$ for the *G. radlkoferi* ethanolic leaf extracts (P001-P005) (Fig. S2A), the *G. flanaganii* ethanolic leaf extracts P157, P159 and P161 (Fig. S2B), and *G. sutherlandii* ethanolic leaf extracts (Fig. S2C).

Quantification of the reference compound 3,5,7-trihydroxyflavone (galangin) was based on the intensity of a black band at $R_f \sim 0.55$ in the UV 254 nm images after development. Galangin was detected in all five of the *G. radlkoferi* extracts (28.48 - 43.69 μg/10 mg, Table 1) (Fig. 3D, tracks 1-5, right). All five *G. flanaganii* extracts contained galangin (38.67 - 73.16 μg/10 mg, Table 1) (Fig. 3E, tracks 1-5, right), as well as all four of the *G. sutherlandii* extracts (16.74 – 25.72 μg/10 mg, Table 1) (Fig. 3F, tracks 1-4, right). In addition, peak profiles showed peaks for the sample tracks that aligned with the reference compound tracks at $R_f \sim 0.55$, corresponding to galangin (Fig. S3). The presence of galangin in sample tracks was supported by the appearance of a mustard yellow band at $R_f \sim 0.55$ in NP-derivatized plates visualised under RT white light (Fig. S4 A-C), and the appearance of a light blue fluorescence in the same zone ($R_f \sim 0.55$) in HPTLC plates derivatized with NP

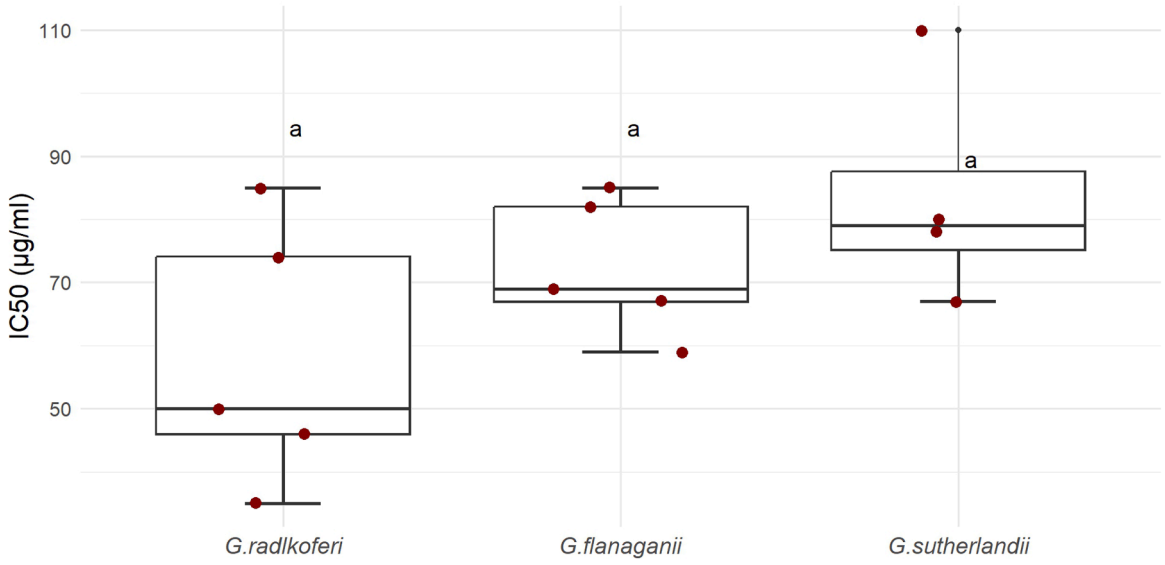


**Fig. 2.** Anti-tyrosinase activities of leaf extracts of wild-growing trees of the three *Greyia* species. Data from four or five biological replicate trees of each species (*G. radlkoferi, G. flanaganii, G. sutherlandii*) are plotted as the $IC_{50}$ [ethanolic leaf extract concentration (µg/mL) that inhibits 50 % of tyrosinase enzyme activity]. The boxes indicate the interquartile range, while the horizontal line within the boxes shows the median. The whisker ends indicate the minimum and maximum values. The $IC_{50}$ values for each tree are indicated with red dots (jitter). Significance is indicated by the letters where samples with the same letter are not significantly different from one another (Tukey's Multiple Comparison Test, alpha = 0.05). The median $IC_{50}$ for *G. radlkoferi* (P001-P005), *G. flanaganii* (P157-P161), *G. sutherlandii* (P241-P244) were 50 µg/mL, 69 µg/mL and 79 µg/mL, respectively.

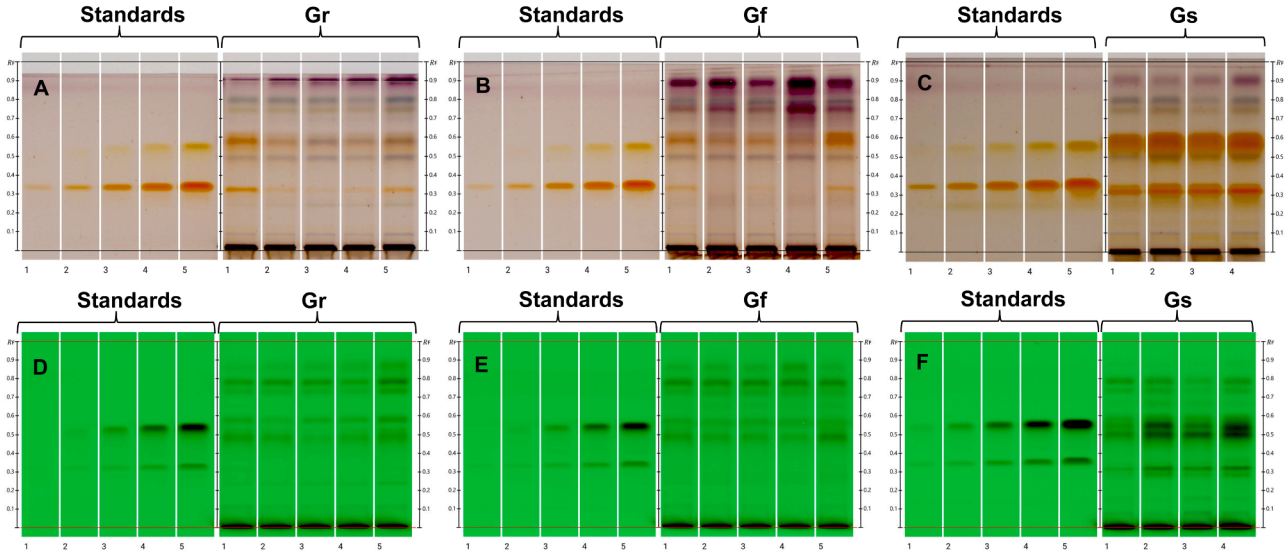


**Fig. 3.** High Performance Thin Layer Chromatography (HPTLC) of *Greyia* leaf extracts to quantify active biomarker compounds. **A, B, C**: Developed HPTLC plates derivatized with natural product reagent and *p*-anisaldehyde illuminated under Remission-Transmission light for visualization of 2',4',6,-trihydroxydihydrochalcone. **D, E, F**: Developed HPTLC plates illuminated under UV light at 254 nm for visualization of 3,5,7-trihydroxyflavone (galagin). For all panels **A-F**, dilution series of a mixture of 2′,4′,6′-trihydroxydihydrochalcone and galagin were loaded in a volume of 10 µL per track with each compound applied from stock concentrations of 31.25, 62.5, 125, 250 and 500 µg/ml (tracks 1-5 on the left), and the ethanolic leaf extracts of *Greyia radlkoferi* (P001-P005) (panel **A** and **D**), *G. flanaganii* (P157 – P161) (panel **B** and **E**) and *Greyia sutherlandii* (P241 – P244) (panel **C** and **F**) were loaded in volumes of 20 uL of 10 mg/mL stock concentrations (tracks 1-5 or 1-4 on the right).

reagent viewed under UV 366 nm (Fig. S4 D-F).

### 3.4. Phylogenetic analysis with standard plant DNA barcoding genes

All of the Bayesian based phylogenetic analyses of individual and combined DNA barcodes (ITS, *matK, trnL-F, psbA-trnH*) for the sampled Geraniales accessions were judged to have converged on the posterior, with estimated sample sizes of over 200 for all parameters. The combined tree is shown in Fig. 4a which also includes information on the *Greyia* barcode sequences deposited at the Barcode of Life database and Genbank. Three major clades are resolved: a *Rhynchotheca/Vivianía/Wendtia/Balbisia* clade, a *Melianthus/Bersama* clade, and a *Francoa/Tetilla/Greyia* clade, consistent with previous research using these markers and with other studies (Linder et al., 2006; Palazzesi et al., 2012). The last clade resolved *Francoa* and *Tetilla* as sister to a monophyletic *Greyia*. Internal relationships within *Greyia* are poorly resolved and branch lengths are extremely short relative to other Geraniales genera, with only *G. flanaganii* being monophyletic with maximal

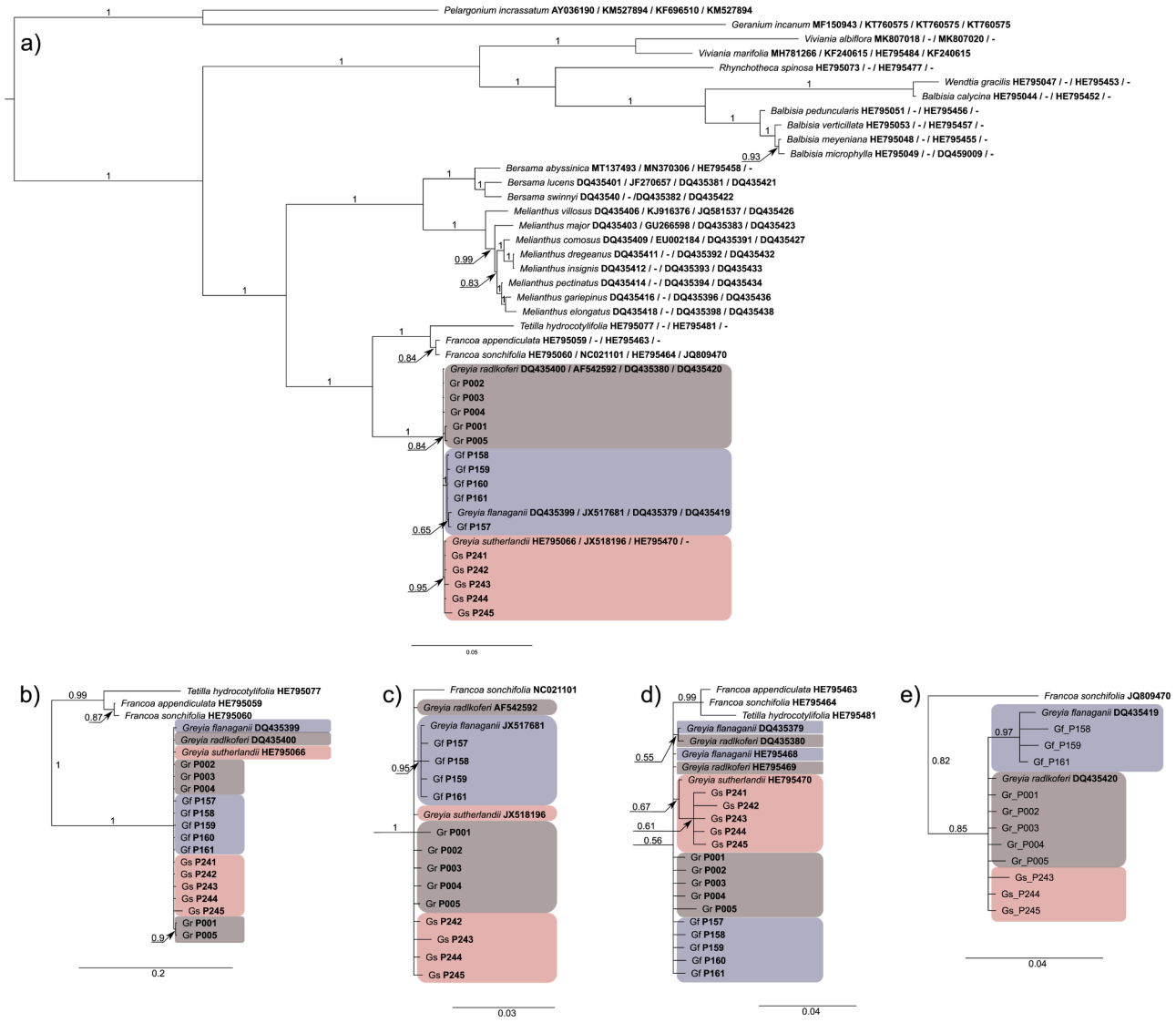


**Fig. 4.** Barcoding phylogenies of the Geraniales including *Greyia* spp. (a) Bayesian 50 % majority-rule consensus phylogeny of the Geraniales using combined barcode sequences of ITS, *matK, trnL-F,* and *psbA-trnH*. Numbers above branches/on arrows are Bayesian posterior probabilities. Scale bars are in number of substitutions per site. Genbank accessions used for each tip are in bold following the tip name. Genbank accessions are listed in the order ITS / *matK* / *trnL-F* / *psbA-trnH*. Unavailable or unsampled barcodes are indicated with a dash. DNA sequences of five trees per core population of *Greyia radlkoferi* (P001-P005), *Greyia sutherlandii* (P241 – P245), and *G. flanaganii* (P157 – P161) are available from https://portal.boldsystems.org (search term = GREY and the qualifier [recordsetcode] from the dropdown menu). The sequences for each barcode for one tree per species have also been submitted to GenBank (ITS - P002: PX210468; P161: PX210469; P244: PX210470; *matK* - P001: PX393127; P161: PX393128; P245: PX393129, *trnL-F* - P002: PX502302; P161: PX502303; P244: PX502304, *psbA-trnH* - P002: PX430637; P161: PX430638; P244: PX430639). Sections of single gene phylogenies based on Bayesian 50 % majority-rule consensus trees are shown for *Greyia* and close relatives with (b) ITS; (c) *matK;* (d) *trnL-F,* and (e) *psbA-trnH* barcodes. The complete Geraniales gene trees for b-e are shown in Figure S5a-d.

support, and *G. sutherlandii* with reasonable support. All individual markers showed similar patterns, if with lower resolution and support (Fig. 4b-e). Only ITS resolved *Greyia* as monophyletic with strong support. *Greyia flanaganii* was monophyletic in *mat*K and *psbA-trnH* trees with reasonable support, but otherwise no strongly supported relationships between *Greyia* individuals were found (complete trees from individual barcodes are available in Fig. S5a-d).

Barcode gap analysis showed that pairwise divergences between barcodes had considerable overlap between intraspecific and interspecific values for ITS. Although differences were observed between intraspecific and interspecific values for *mat*K and *trn*L-F, interspecific differences were bimodal with peaks at zero and the maximum observed value. Only *psb*A-*trn*H showing interspecific values well above the threshold of 0.01 (primarily driven by the *G. flanaganii* sequences; see Table S2). Consistent with the above, all threshID() calls for addressing the barcoding gap were "ambiguous" except for the *psbA-trnH* sequences of *G. flanaganii*.

## 4. Discussion

Previous work on *Greyia* medicinal activity and DNA barcoding was limited to a small number of individuals grown in botanical gardens and lacking provenance data (Lall et al., 2016; Linder et al., 2006; Mapunya et al., 2011). This study set out to address this limitation by sampling from wild-growing trees from geographically and morphologically representative populations of each of the three species. The main findings were that ethanolic leaf extracts from wild-growing *G. radlkoferi* and *G. flanaganii* exhibited anti-tyrosinase activities that were equivalent to extracts from botanical garden trees reported previously. *Greyia sutherlandii* trees growing in their native habitat in the Drakensberg,

KwaZulu-Natal Province had similar leaf anti-tyrosinase activity to the sampled populations of *G. radlkoferi* trees in Limpopo Province and *G. flanaganii* in the Eastern Cape Province (Fig. 2). The assay results were supported by HPTLC results which showed the presence of the main active compound 2'4'6'-trihydroxydihydrochalcone in the extracts from all three species, with the exception of two trees.

In addition, we evaluated DNA barcoding to differentiate the *Greyia* species in general as well as to assist production orchard growers where the overlap in flower and leaf morphology traits poses a problem for identification. Phylogenetic analysis using ITS, *trnL-F, matK* and *psbA-trnH* showed clear differentiation from other genera in the order *Geraniales*. However, there were insufficient polymorphisms across all four barcodes within *Greyia*, resulting in unresolved interspecific relationships and the uncertain monophyly of *G. radlkoferi*.

The levels of anti-tyrosinase activity from the ethanolic leaf extracts of wild-growing *G. radlkoferi* and *G. flanaganii* trees were in the same range as previously reported for individual trees of each respective species which were collected from the Manie Van der Schiff Botanical Garden (University of Pretoria). The average $IC_{50}$ value for the five *G. radlkoferi* trees in the Limpopo province was 58 μg/mL, comparable with 17.96 μg/mL from the individual botanical garden tree reported by Lall et al. (2016). The five *G. flanaganii* trees in Eastern Cape Province had an average $IC_{50}$ of 72 μg/ml in our study, comparable with 32.62 μg/mL for the individual cultivated tree (Mapunya et al., 2011). Anti-tyrosinase activity of extracts from a *Greyia* orchard in the Gauteng Province varied widely from 20-160 μg/ml (Ing et al., 2020). The authors used morphological traits to allocate putative species identities to these orchard trees of unknown provenance, which were sourced from local nurseries. However, there was no correlation of activity with their "species" morphotypes (Ing et al., 2020). In another study focussed on glasshouse grown *Greyia* plants derived from the seed of a *G. radlkoferi* tree from this orchard, the 50 % inhibitory concentrations for anti-tyrosinase activity were between 20-50 μg/ml (Malele et al., 2024).

The *Greyia* extracts in this study exhibited similar anti-tyrosinase activities to that reported from extracts of other African plants, for example *Combretum collinum* Fresen., *Schotia brachypetala* Sond., and *Vachelia nilotica* (L.) P.J.H. Hurter & Mabb. plant extracts which exhibited $IC_{50}$ values of 35.07 μg/mL, 47.92 μg/mL and 12.97 μg/mL, respectively (Lall et al., 2019). Other examples of plants with anti-tyrosinase activity include *Oncosiphon suffruticosum* (L.) Källersjö with an $IC_{50}$ of 61.46 μg/mL (Adewinogo et al., 2021), *Hyaenanche globosa* Lamb with an $IC_{50}$ of 180.80 μg/mL (Momtaz et al., 2010), *Aloe ferox* (138.20 μg/ mL) and *Aloe spectabilis* (78.90 μg/mL) (Mikayoulou et al., 2021).

Ethanolic leaf extracts from *G. radlkoferi* and *G. flanaganii* exhibited low toxicity to mammalian cells, making them good candidates for a skincare product development (Mapunya et al. 2011; Lall et al. 2016). These studies also reported isolation and identification of the main active compound as 2',4',6'-trihydroxydihydrochalcone with an $IC_{50}$ value of 69.15 μM (17.70 μg/mL) (Lall et al., 2016) and 69.10 μM (17.86 μg/mL) (Mapunya et al., 2011). A second compound with anti-tyrosinase activity, 3,5,7-trihydroxyflavone (galangin), was also purified from the *G. radlkoferi*, however its $IC_{50}$ value of 420 μM (113.60 μg/mL) indicates a minor contribution to the overall extract activity (Lall et al., 2016).

Our study supported the conclusion that 2',4',6'-trihydroxydihydrochalcone was the main contributor to anti-tyrosinase activity in *Greyia* extracts, as this compound was quantified by HPTLC at levels up to 19.69, 11.59 and 30.28 μg/10 mg extract in the wild-growing *G. radlkoferi, G. flanaganii* and *G. sutherlandii* samples, respectively, without tailing effects being observed (Table 1 and Fig. 2). The HPTLC analysis (UV 254 nm light) was able to quantify galagin in the *Greyia* extracts at levels of 16.74 – 73.16 ug/ 10 mg extract (Table 1). Although galangin has weak anti-tyrosinase activity, it would be interesting to determine the combinational effects of galangin and 2',4',6'-trihydroxydihydrochalcone to determine whether there are any antagonistic or synergistic effects between these two metabolites.

Herbarium records of *Greyia* species show distribution ranges with *G. flanaganii* being an Eastern Cape species, *G. sutherlandii* mostly a KwaZulu-Natal species and *G. radlkoferi* mainly a Limpopo species (Fig. 1). There was overlap of species ranges of *G. sutherlandii* and *G. radlkoferi* in Mpumalanga, but also several records that were out of place for example *G. sutherlandii* and *G. radlkoferi* records in Eastern Cape, and *G. sutherlandii* records in Limpopo. We contend that this may be due to misidentifications between the deciduous *G. sutherlandii* and *G. radlkoferi* species or cultivated individuals, since sampling of inflorescences may have been at a time when only leaf flush was occurring, resulting in confusion between woolly/hairy and glabrous species, as pointed out by Steyn (1974). Furthermore, the lack of obvious flower morphological differences and acropetal development of the inflorescences of *G. sutherlandii* and *G. radlkoferi* can result in mis-identifications when sampled at different stages of inflorescence development. *Greyia* production orchards have a similar identification problem (Ing et al 2020), and DNA barcoding was therefore evaluated to differentiate species.

Even with the addition of two extra barcodes and multiple individuals, the findings from our study show that single or combined DNA barcodes (ITS, *trnL-F, matK, psbA-trnH*) were unable to differentiate natural populations of the three *Greyia* species. This may be explained by the recent divergence within this genus. First, the combined Geraniales phylogenetic tree with the single nuclear and three plastid barcodes from our study (Fig. 4) is consistent with the phylogeny of Palasezzi et al. (2012) based on ITS and *trnL-F*. The sister genera to *Greyia* are *Francoa* and *Tetilla* from Chile in South America, with the other African genera *Melianthus* and *Bersama* as separate clades. Second, attempts to date the historical divergence within the order Geraniales as a whole using DNA data and fossil calibrations support recent diversification of the *Greyia* species from the late Pliocene (~3.2 million years ago (Mya)) (Palazzesi et al., 2012; Sytsma et al., 2014). The study by Linder et al. (2006) was focused on the genus *Melianthus* but used *Greyia* as an outgroup. Their most relevant finding to the current study was that diversification of *Melianthus* and related genera may have been driven by aridification in southern Africa which began in the late Miocene over the past 20 million years. Palasezzi et al. (2012) used new fossil evidence in the Viviana lineage together with ITS and *trnL-F* data, and estimated divergence of the Melianthaceae from the Francoaceae (including *Greyia*) at 32 Mya, and Francoa from *Greyia* at 11.2 Mya. Sytsma et al. (2014) argued on technical grounds that these divergence times were earlier by about 10 million years. While these dating attempts remain controversial with large confidence intervals, the relationships between the genera are consistent, and both authors support recent diversification of the *Greyia* species. However, the DNA data resolution and lack of any *Greyia* fossil evidence prevents dating the divergence within the genus.

*Greyia flanaganii* DNA barcode data for the plastid gene regions of *matK* and *psbA-trnH* exhibited several polymorphisms with the other two species, resulting in a monophyletic *G. flanaganii* lineage with maximal posterior probability in the Bayesian phylogenetic trees (Fig. 4). This was also evident in previous phylogenies (Palazzesi et al., 2012; Sytsma et al., 2014). Considering the difference in flower morphology between *G. flanaganii* and the other two species, its evergreen habit, and these plastid polymorphisms, the identification of *G. flanaganii* in production orchards should be possible. *G. flanaganii* has a current distribution west of the Kei River in the Eastern Cape and is confined to low altitude (<1000 masl) grasslands, and is described as more drought tolerant than the other two species (Mbambezeli, 2002). The closed bell-shaped flowers of *G. flanaganii* compared to the open flowers of the other two species (Fig. 1) may also indicate selection for different pollinators. Thus, the niche and geographic isolation of *G. flanaganii* may have contributed to its divergence from the other two *Greyia* species.

The difficulty in differentiating *G. sutherlandii* from *G. radlkoferi* using DNA barcodes in our study reflects the challenges experienced by

researchers in the search for universal DNA barcode(s) for plants, especially between closely related taxa. There have been many attempts at evaluating combinations of plastid gene regions and/or nuclear gene regions (Hollingsworth et al., 2016). The International Barcode of Life consortium initially recommended the use of *matK* and *rbcL* in plants, however these lacked species-level resolution in a range of lineages (CBOL-Plant-Working-Group, 2009). As seen in our study, there were insufficient *matK* polymorphisms to differentiate *G. radlkoferi* from *G. sutherlandii* (Fig. 4c; Fig. S5b). We did not include *rbcL* in our study since the GenBank sequences for each *Greyia* species did not add a significant number of polymorphisms. The CBOL included a trial period of testing other barcodes, namely *psbA-trnH* and ITS (Hollingsworth, 2011), which were two of the additional barcodes used in this study. Both barcodes improved the differentiation between the genera *Greyia* and *Francoa*, however ITS did not distinguish the three *Greyia* species (Fig. 4b; Fig. S5a). This is contrary to other studies where species discrimination success was improved from 50-62 % to 77-82 % when ITS was combined with two plastid markers (Hollingsworth, 2011). The *psbA-trnH* barcode did differentiate *G. flanaganii* from the other two *Greyia* species (Fig. 4e; Fig. S5d).

Another consideration in using ITS as a DNA barcode is that rDNA occurs in hundreds to thousands of copies in plant genomes (Poczai and Hyvönen, 2010). This subjects the region to concerted evolution - a process in which the sequences of the tandem repeats become homogenized after a hybridization event (Koch et al., 2003). Over many generations, this process can lead to the complete loss of the ancestral signal at a particular nucleotide position of ITS, for example. In this study we evaluated a relevant polymorphic ITS site which was a T nucleotide in *G. radlkoferi* (position 401 in HE795065), and a C in *G. sutherlandii* (position 401 in HE795066). All five *G. radlkoferi* trees from Limpopo had the T nucleotide at this position, however two of the *G. sutherlandii* trees from KwaZulu-Natal had the C nucleotide (P241, P245) and three of the trees (P242, P243, P244) were heterozygous (Y) at this position. This may represent incomplete concerted evolution where unequal crossing over and gene conversion is not complete (Xu et al., 2017), leaving remnants of the original sequence - further evidence of recent divergence of these species.

DNA barcoding requires a sufficient "barcode gap", which is fulfilled when the interspecific genetic distances exceed intraspecific variation (CBOL-Plant-Working-Group, 2009). Several approaches have been used to quantify the barcode gap, such as calculating whether the maximum Kimura 2 Parameter (K2P) intraspecific distances were lower than the minimum interspecific distance (Caetano Wyler and Naciri, 2016). Song et al. (2023) obtained a 72 % species identification success rate in the Peruvian Lomas flora for *matK, rbcL* and ITS when applying this method, which was improved slightly to 76 % using a phylogenetic tree-based method.

We acknowledge that our selection of five species-representative *Greyia* individuals from each geographic site plus the one or two Genbank sequences of *Greyia* with unknown provenances do not cover the complete intraspecies diversity. Nevertheless, the individual or combined phylogenetic tree analyses indicated insufficient barcode gaps for the tested nuclear and plastid barcodes, making these markers suboptimal for identifying *Greyia spp*. On the whole, *G. flanaganii* seems to be the most differentiated from the other two species with the barcodes used in this study, but only using *psbA-trnH* under default pairwise divergence cutoffs.

DNA barcoding has proven to be challenging in recently diverged lineages or flora, as seen in our study of *Greyia*. A case in point is the flora of Hawaii. Since the islands are isolated and less than five million years old, current plant lineages arrived by migration, followed by rapid diversification. DNA barcoding with ITS and four plastid genes of a range of taxa across the islands yielded species identification success rates of less than 22 % (Stallman et al., 2019). DNA barcoding can also fail in taxa where there is a high level of hybridization, for example in the genus *Salix* L. (willow) a comparison of plastid barcodes across 150 species showed the dominance of a single haplotype (Percy et al., 2014). This analysis pointed to hybridization and surprisingly, a selective sweep acting on the plastid genome. The authors used molecular dating to show that this event was recent, thus ruling out incomplete lineage sorting.

Future work to resolve the molecular systematics of the genus *Greyia* would likely require the use of a larger number of phylogenetically informative SNP markers acquired through genomic technologies (Daru et al., 2016). One approach could compare whole chloroplast sequences with the aim of finding alternative DNA barcodes, however the slow rate of change of plastid sequences is not ideal for recently diverged taxa, as seen in a study of the genus *Amaranthus* L. (Viljoen et al., 2018). Genome skimming is an alternative method to obtain larger numbers of informative plastid and nuclear ribosomal RNA (nrRNA) SNPs. This was implemented in the tree genus *Acer*, where plastid phylogenies do not differentiate species well (Fu et al., 2024). However, there were some cases of discordance between the *Acer* L. plastome and nuclear ribosomal phylogenies (Fu et al., 2024), which highlights the problem caused in some lineages due to hybridization and chloroplast capture.

Recent plant molecular systematic studies have explored the use of genome-wide SNP markers obtained through Illumina sequencing of total genomic DNA, or reduced representation methods known as genotyping by sequencing or RADseq (Andrews et al., 2016). The latter approaches avoid the problem of repetitive DNA and plants with large genomes. These methods can be used for SNP discovery followed by development of a SNP panel for species differentiation, as conducted in the genus *Vitis* L. (Myles et al., 2010). Such a method could be employed to differentiate unknown *Greyia* species in production orchards. Alternatively, panels of single copy protein coding genes or adjacent introns/non-coding regions can be used to extract SNP data for molecular phylogenomics, as illustrated with mRNA data in the 1KP project (Leebens-Mack and One Thousand Plant Transcriptomes Initiative, 2019) or using the Angiosperms 353 panel recently implemented for Angiosperm phylogenomics (Zuntini et al., 2024). These offer promising alternatives for "barcoding" individual *Greyia* trees, and also for exploring phylogenetic relationships and taxonomic implications in this recently radiated group.

In conclusion, our study shows for the first time that *Greyia* trees of all three species growing in their natural environment have potent anti-tyrosinase activity and contain the active compound 2',4',6'-trihydroxydihydrochalcone in their leaves. This means that *G. sutherlandii*, in addition to *G. radlkoferi* and *G. flanaganii* can be used as source material as cuttings for production orchards (Malele et al., 2021). This would facilitate the scale-up of commercial production of herbal remedies for skin hyper-pigmentation. This manuscript also contributes to quality control and the prevention of adulteration of these products since we provide an HPTLC protocol for detection of the main active compound 2',4',6'-trihydroxydihydrochalcone.

From a biodiversity point of view, authorities in KwaZulu-Natal and Mpumalanga Provinces, where *G. sutherlandii* is distributed, would need to be alert to unregulated harvesting from wild-growing trees. The evolutionary conservation of these compounds in the *Greyia* genus points to their functional importance. This genus has previously been flagged for its interesting flavanoid profiles (Bohm and Chan, 1992). Thus, future work could explore hypotheses about the roles of these compounds in either stress tolerance or as anti-herbivory/anti-microbial agents.

Another important contribution of our study was the evaluation of four standard DNA barcode markers ITS, *matK, trnL-F*, and *psbA-trnH* for *Greyia*, which had not been done before. We contend that our strategy of sampling from "core populations" located close to the three provenances of the original type specimens was the best strategy to link DNA data to species descriptions with the limited resources available. The outcomes were that we identified a small number of "species-specific" SNPs, and there was evidence of a barcode gap for *psbA-trnH* between *G. flanaganii* and the other two species. However, rigorous phylogenetic analysis with

these four barcode markers failed to differentiate the three species with confidence, pointing to the relatively recent divergence of this taxon as previously proposed (Palazzesi et al., 2012).

These findings have implications for both using barcoding in *Greyia* for biodiversity monitoring, and *Greyia* systematics. First, similar to other taxons where standard barcodes were insufficient (Percy et al., 2014), future work would likely depend on genomics approaches to understand the evolutionary divergence of the species and identify additional barcodes. Approaches such as whole chloroplast sequencing, genome skimming or whole genome SNP analysis would be required. Second, to address the taxonomic revision of the genus *Greyia* it will be necessary to find congruence between the morphological and phylogenetic species concepts. Our collections plus the herbarium specimens in national herbaria (Fig. 1A) will facilitate a comprehensive morphometrics assessment of the genus. Molecular phylogenomics using panels of informative protein-coding gene markers is likely to be the best approach to resolve *Greyia* species and higher order relationships at the DNA level.

Finally, a limitation of our study was sampling from only one population per *Greyia* species, which may not have captured the inter- and intraspecific range of medicinal activity or genetic diversity in South Africa and Eswatini. This is especially important considering the partial overlap in distribution of *G. radlkoferi* and *G. sutherlandii* (Fig. 1A), and difficulty in differentiating them in the field. Therefore, ongoing future work would require widespread sampling and resource-efficient population genomics approaches to screen plants for medicinal activity and identify and apply novel barcodes.

## Funding sources

The research was supported by funding from the NRF Foundational Biodiversity Information Programme grant to DKB (FBIS2204041924), NRF SARChI grant to NL (SARCI150227114490), a DSTI grant to NL (DSTI/CON 3911/2025), a NRF SARChI grantholder-linked scholarship to IB (98334), and Oppenheimer Memorial Trust Awards to DKB (23-1431) and JB (24-5181).

## Data availability statement

DNA barcode sequences are available from the Barcode of Life database https://portal.boldsystems.org/, and representative sequences from each *Greyia* species have also been deposited at Genbank.

## CRediT authorship contribution statement

**Iné Botha:** Writing – original draft, Methodology, Investigation, Formal analysis, Data curation. **Marco N. De Canha:** Writing – review & editing, Visualization, Supervision, Methodology, Formal analysis. **Kenneth Oberlander:** Writing – review & editing, Visualization, Methodology, Formal analysis. **Jana Botes:** Writing – review & editing, Methodology, Investigation, Formal analysis. **Namrita Lall:** Writing – review & editing, Supervision, Resources, Funding acquisition. **Dave K. Berger:** Writing – review & editing, Writing – original draft, Visualization, Supervision, Resources, Project administration, Funding acquisition, Data curation, Conceptualization.

## Declaration of competing interest

The authors declare that they have no known competing financial interests or personal relationships that could have appeared to influence the work reported in this paper.

## Acknowledgements

The authors acknowledge the following field workers who assisted in identifying *Greyia* populations and/or sampling: Neil Potter, Trystan Nadasen, Arnold Frisby, Jeff Morris, Christina Potgieter, Mark Robertson (Ezemvelo KZN Wildlife), Wiam Haddad (ZZ2). *Greyia* sampling was conducted with research permits issued by the Limpopo Economic Development, Environment and Tourism, Ezemvelo KZN Wildlife, and the Eastern Cape Economic Development, Environment Affairs and Tourism. This research was conducted under the BABS (Bioprospecting, Access and Benefit Sharing) Permit Number BP 201713 (Department of Environment, Forestry and Fisheries). We thank Monique Botha for Fig. 1A. We acknowledge the use of the Biosecurity App, developed and maintained by Biosyntrix, South Africa (https://biosyntrix.co.za/), for facilitating field data collection and sample management of the *Greyia* tree populations.

## Supplementary materials

Supplementary material associated with this article can be found, in the online version, at doi:10.1016/j.sajb.2025.11.035.

## References

Adewinogo, S.O., Sharma, R., Africa, C.W.J., Marnewick, J.L., Hussein, A.A., 2021. Chemical composition and cosmeceutical potential of the essential oil of *Oncosiphon suffruticosum* (L.) Kallersjo. Plants 10, 1315.

Andrews, K.R., Good, J.M., Miller, M.R., Luikart, G., Hohenlohe, P.A., 2016. Harnessing the power of RADseq for ecological and evolutionary genomics. Nat. Rev. Genet. 17, 81–92. https://www.ncbi.nlm.nih.gov/pubmed/26729255.

Baldwin, B., Sanderson, M., Porter, J., Wojciechowski, M., Campbell, C., Donoghue, M., 1995. The ITS Region of Nuclear Ribosomal DNA: A Valuable Source of Evidence on Angiosperm Phylogeny. Ann. Missouri Botan Garden 82, 247–277. https://doi.org/10.2307/2399880.

Bass, E., 2022. ggtukey: Compact Letter Displays for 'ggplot2' (v0.4.0). https://ethanbass.github.io/ggtukey/. Date accessed 3 November 2025.

Bohm, B.A., Chan, J., 1992. Flavonoids and Affinities of *Greyiaceae* with a Discussion of the Occurrence of B-Ring Deoxyflavonoids in Dicotyledonous Families. Syst. Bot. 17, 272–281. http://www.jstor.org/stable/2419522.

Brown, S.D.J., Collins, R.A., Boyer, S., Lefort, M.-C., Malumbres-Olarte, J., Vink, C.J., Cruickshank, R.H., 2012. Spider: An R package for the analysis of species identity and evolution, with particular reference to DNA barcoding. Mol. Ecol. Resour. 12, 562–565. https://onlinelibrary.wiley.com/doi/abs/10.1111/j.1755-0998.2011.03108.x.

Byrne, M., Macdonald, B., Francki, M., 2001. Incorporation of Sodium Sulfite into Extraction Protocol Minimizes Degradation of *Acacia* DNA. Biotechniques 30, 742–748. https://doi.org/10.2144/01304bm06.

Caetano Wyler, S., Naciri, Y., 2016. Evolutionary histories determine DNA barcoding success in vascular plants: seven case studies using intraspecific broad sampling of closely related species. BMC. Evol. Biol. 16, 103. https://doi.org/10.1186/s12862-016-0678-0.

CBOL-Plant-Working-Group, 2009. A DNA barcode for land plants. Proc. Natl. Acad. Sci. 106, 12794–12797. https://www.pnas.org/content/pnas/106/31/12794.full.pdf.

Chen, S., Yao, H., Han, J., Liu, C., Song, J., Shi, L., Zhu, Y., Ma, X., Gao, T., Pang, X., Luo, K., Li, Y., Li, X., Jia, X., Lin, Y., Leon, C., 2010. Validation of the ITS2 Region as a Novel DNA Barcode for Identifying Medicinal Plant Species. PLoS. One 5, e8613. https://doi.org/10.1371/journal.pone.0008613.

Dahlgren, R., Van Wyk, A.E., 1988. Structures and relationships of families endemic to or centered in Southern Africa. Monogr. Syst. Bot. Missouri Bot. Gard. 25, 1–94.

Daru, B.H., Berger, D.K., van Wyk, A.E., 2016. Opportunities for unlocking the potential of genomics for African trees. New Phytologist 210, 772–778. https://doi.org/10.1111/nph.13826.

De la Cruz, P., 2016. *Greyia radlkoferi*. South African National Biodiversity Institute (SANBI). http://pza.sanbi.org/greyia-radlkoferi. Accessed 17 June 2025.

Fu, N., Xu, Y., Jin, L., Xiao, T.W., Song, F., Yan, H.F., Chen, Y.S., Ge, X.J., 2024. Testing plastomes and nuclear ribosomal DNA sequences as the next-generation DNA barcodes for species identification and phylogenetic analysis in *Acer*. BMC. Plant Biol. 24, 445. https://www.ncbi.nlm.nih.gov/pubmed/38778277.

Hall, T.J., 1999. BioEdit: a user-friendly biological sequence alignment editor and analysis program for Windows 95/98/NT. Nucleic. Acids. Symp. Ser. 41, 95–98.

Harvey, W.H., 1859. *Greyia* Hook. & Harv. University Press (MH Gill), Trinity College (Ireland). https://books.google.co.za/books?id=gdBQAQAAMAAJ&dq.

Hollingsworth, P.M., 2011. Refining the DNA barcode for land plants. Proc. Natl. Acad. Sci. U. S. A 108, 19451–19452. https://www.ncbi.nlm.nih.gov/pubmed/22109553.

Hollingsworth, P.M., Li, D.Z., van der Bank, M., Twyford, A.D., 2016. Telling plant species apart with DNA: from barcodes to genomes. Philos. Trans. R. Soc. Lond. B Biol. Sci. 371. https://www.ncbi.nlm.nih.gov/pubmed/27481790.

Hooker, W.J., 1895. *Greyia flanaganii* Bolus Plate 2349, Hookers Icones Plantarum. Longman, London. https://www.biodiversitylibrary.org/page/16232426.

Ing, V., Kleynhans, R., Prinsloo, G., 2020. Morphological, phenological and metabolomic profiling of Greyia species. Acta Hortic. 49–56. https://doi.org/10.17660/ActaHortic.2020.1287.7.

Killick, D.J.B., Kimpton, J., 1977. Plate 1732. *Greyia sutherlandii* Hook & Harv., Flowering Plants of Africa. National Botanical Institute, Johannesburg, pp. 1–4.

Koch, M.A., Dobeš, C., Mitchell-Olds, T., 2003. Multiple Hybrid Formation in Natural Populations: Concerted Evolution of the Internal Transcribed Spacer of Nuclear Ribosomal DNA (ITS) in North American *Arabis divaricarpa* (*Brassicaceae*). Mol. Biol. Evol. 20, 338–350. https://doi.org/10.1093/molbev/msg046.

Kress, W.J., 2017. Plant DNA barcodes: Applications today and in the future. J. Syst. Evol. 55, 291–307. https://doi.org/10.1111/jse.12254.

Kress, W.J., Erickson, D.L., 2008. DNA barcodes: Genes, genomics, and bioinformatics. Proc. Natl. Acad. Sci. 105, 2761–2762. https://doi.org/10.1073/pnas.0800476105.

Krishna Krishnamurthy, P., Francis, R.A., 2012. A critical review on the utility of DNA barcoding in biodiversity conservation. Biodivers. Conserv. 21, 1901–1919. https://link.springer.com/article/10.1007/s10531-012-0306-2.

Lall, N., 2019. Underexplored Medicinal Plants from Sub-Saharan Africa: Plants with Therapeutic Potential for Human Health. Elsevier Science (Academic Press), p. 358pp. https://books.google.co.za/books?id=PQq9DwAAQBAJ.

Lall, N., Mogapi, E., de Canha, M.N., Crampton, B., Nqephe, M., Hussein, A.A., Kumar, V., 2016. Insights into tyrosinase inhibition by compounds isolated from *Greyia radlkoferi* Szyszyl using biological activity, molecular docking and gene expression analysis. Bioorg. Med. Chem. 24, 5953–5959. https://www.sciencedirect.com/science/article/pii/S0968089616307878.

Lall, N., van Staden, A.B., Rademan, S., Lambrechts, I., De Canha, M.N., Mahore, J., Winterboer, S., Twilley, D., 2019. Antityrosinase and anti-acne potential of plants traditionally used in the Jongilanga community in Mpumalanga. South Afr. J. Botany 126, 241–249. https://doi.org/10.1016/j.sajb.2019.07.015.

Leebens-Mack, J.H., One Thousand Plant Transcriptomes Initiative, 2019. One thousand plant transcriptomes and the phylogenomics of green plants. Nature 574, 679–685. https://doi.org/10.1038/s41586-019-1693-2.

Linder, H.P., Dlamini, T., Henning, J., Verboom, G.A., 2006. The evolutionary history of *Melianthus* (Melianthaceae). Am. J. Bot. 93, 1052–1064. https://doi.org/10.3732/ajb.93.7.1052.

Malele, J., Kleynhans, R., Prinsloo, G., Matsiliza-Mlathi, B., 2021. Optimizing the cutting production of *Greyia radlkoferi*. South Afr. J. Botany 142, 293–298. https://www.sciencedirect.com/science/article/pii/S0254629921002556.

Malele, J., Kleynhans, R., Prinsloo, G., Matsiliza-Mlathi, B., 2024. Metabolomic profiling of *Greyia radlkoferi* on water stress, phenological growth stages, and leaf age using 1H NMR. South Afr. J. Botany 173, 147–158. https://www.sciencedirect.com/science/article/abs/pii/S0254629924005118.

Mapunya, M.B., Hussein, A.A., Rodriguez, B., Lall, N., 2011. Tyrosinase activity of *Greyia flanaganii* (Bolus) constituents. Phytomedicine 18, 1006–1012. https://www.sciencedirect.com/science/article/pii/S0944711311001255.

Mbambezeli, G., 2002. *Greyia flanaganii*. South African National Biodiversity Institute (SANBI). http://pza.sanbi.org/greyia-flanaganii. Accessed 10 September 2021.

Mbambezeli, G., 2016. *Greyia sutherlandii*. South African National Biodiversity Institute (SANBI). http://pza.sanbi.org/greyia-sutherlandii. Accessed 17 June 2025.

Meisel, B., Korsman, J., Kloppers, F.J., Berger, D.K., 2009. *Cercospora zeina* is the causal agent of grey leaf spot disease of maize in southern Africa. Eur. J. Plant Pathol. 124, 577–583. https://doi.org/10.1007/s10658-009-9443-1.

Michiels, A., Van den Ende, W., Tucker, M., Van Riet, L., Van Laere, A., 2003. Extraction of high-quality genomic DNA from latex-containing plants. Anal. Biochem. 315, 85–89. https://www.sciencedirect.com/science/article/abs/pii/S0003269702006656.

Mikayoulou, M., Mayr, F., Temml, V., Pandian, A., Vermaak, I., Chen, W., Komane, B., Stuppner, H., Viljoen, A., 2021. Anti-tyrosinase activity of South African *Aloe* species and isolated compounds plicataloside and aloesin. Fitoterapia 150, 104828. https://www.sciencedirect.com/science/article/pii/S0367326X21000034.

Momtaz, S., Lall, N., Hussein, A., Ostad, S.N., Abdollahi, M., 2010. Investigation of the possible biological activities of a poisonous South African plant; *Hyaenanche globosa* (*Euphorbiaceae*). Pharmacogn. Mag. 6, 34–41. https://phcog.com/article/view/2010/6/21/34-41.

Myles, S., Chia, J.-M., Hurwitz, B., Simon, C., Zhong, G.Y., Buckler, E., Ware, D., 2010. Rapid Genomic Characterization of the Genus *Vitis*. PLoS. One 5, e8219. https://doi.org/10.1371/journal.pone.0008219.

Palazzesi, L., Gottschling, M., Barreda, V., Weigend, M., 2012. First Miocene fossils of Vivianiaceae shed new light on phylogeny, divergence times, and historical biogeography of Geraniales. Biol. J. Linnean Soc. 107, 67–85. https://onlinelibrary.wiley.com/doi/abs/10.1111/j.1095-8312.2012.01910.x.

Percy, D.M., Argus, G.W., Cronk, Q.C., Fazekas, A.J., Kesanakurti, P.R., Burgess, K.S., Husband, B.C., Newmaster, S.G., Barrett, S.C.H., Graham, S.W., 2014. Understanding the spectacular failure of DNA barcoding in willows (*Salix*): Does this result from a trans-specific selective sweep? Mol. Ecol. 23, 4737–4756. https://onlinelibrary.wiley.com/doi/abs/10.1111/mec.12837.

Phillips, E.P., Gower, S., 1923. Plate 101. *Greyia radlkoferi*. In: Pole Evans, I.B. (Ed.), The Flowering Plants of South Africa, The Flowering Plants of South Africa, III. The Speciality Press of South Africa, Ltd., Johannesburg, pp. 1–3.

Poczai, P., Hyvönen, J., 2010. Nuclear ribosomal spacer regions in plant phylogenetics: problems and prospects. Mol. Biol. Rep. 37, 1897–1912. https://doi.org/10.1007/s11033-009-9630-3.

R Core Team, 2024. R: A Language and Environment for Statistical Computing. R Foundation for Statistical Computing, Vienna, Austria. https://www.R-project.org/.

Raclariu, A.C., Heinrich, M., Ichim, M.C., de Boer, H., 2018. Benefits and Limitations of DNA Barcoding and Metabarcoding in Herbal Product Authentication. Phytochem. Anal. 29, 123–128. https://www.ncbi.nlm.nih.gov/pubmed/28906059.

Rambaut, A., Drummond, A.J., Xie, D., Baele, G., Suchard, M.A., 2018. Posterior Summarization in Bayesian Phylogenetics Using Tracer 1.7. Syst. Biol. 67, 901–904. https://doi.org/10.1093/sysbio/syy032.

Ratnasingham, S., Wei, C., Chan, D., Agda, J., Agda, J., Ballesteros-Mejia, L., Boutou, H. A., El Bastami, Z.M., Ma, E., Manjunath, R., Rea, D., Ho, C., Telfer, A., McKeowan, J., Rahulan, M., Steinke, C., Dorsheimer, J., Milton, M., Hebert, P.D.N., 2024. BOLD v4: A Centralized Bioinformatics Platform for DNA-Based Biodiversity Data. In: DeSalle, R. (Ed.), DNA Barcoding: Methods and Protocols. Springer US, New York, NY, pp. 403–441. https://doi.org/10.1007/978-1-0716-3581-0_26.

Rattray, R.D., Stewart, R.D., Niemann, H.J., Olaniyan, O.D., van der Bank, M., 2024. Leafing through genetic barcodes: An assessment of 14 years of plant DNA barcoding in South Africa. South Afr. J. Botany 172, 474–487. https://www.sciencedirect.com/science/article/pii/S0254629924004630.

Ronquist, F., Teslenko, M., van der Mark, P., Ayres, D.L., Darling, A., Höhna, S., Larget, B., Liu, L., Suchard, M.A., Huelsenbeck, J.P., 2012. MrBayes 3.2: Efficient Bayesian Phylogenetic Inference and Model Choice Across a Large Model Space. Syst. Biol. 61, 539–542. https://doi.org/10.1093/sysbio/sys029.

Ronse Decraene, L.P., Smets, E.F., 1999. Similarities in Floral Ontogeny and Anatomy between the Genera *Francoa* (Francoaceae) and *Greyia* (Greyiaceae). Int. J. Plant Sci. 160, 377–393. http://www.jstor.org/stable/10.1086/314123.

SANBI, 2024. Priority plant genera for revision 2024. South African National Biodiversity Institute (SANBI). https://www.sanbi.org/biodiversity/foundations/biosystematics-collections/biosystematics-strategies/. Accessed 2 November 2025.

Sang, T., Crawford, D.J., Stuessy, T.F., 1997. Chloroplast DNA phylogeny, reticulate evolution, and biogeography of *Paeonia* (Paeoniaceae). Am. J. Bot. 84, 1120–1136. https://bsapubs.onlinelibrary.wiley.com/doi/abs/10.2307/2446155.

Schmidt, E., Lotter, M., McCleland, W., 2002. Trees and Shrubs of Mpumalanga and Kruger National Park. Jacana, Johannesburg, South Africa.

Song, F., Deng, Y.-F., Yan, H.-F., Lin, Z.-L., Delgado, A., Trinidad, H., Gonzales-Arce, P., Riva, S., Cano-Echevarría, A., Ramos, E., Aroni, Y.P., Rivera, S., Arakaki, M., Ge, X.-J., 2023. Flora diversity survey and establishment of a plant DNA barcode database of Lomas ecosystems in Peru. Sci. Data 10, 294. https://doi.org/10.1038/s41597-023-02206-y.

Stallman, J.K., Funk, V.A., Price, J.P., Knope, M.L., 2019. DNA barcodes fail to accurately differentiate species in Hawaiian plant lineages. Botan. J. Linnean Soc. 190, 374–388. https://doi.org/10.1093/botlinnean/boz024.

Jr Stewart, C.N., Via, L.E., 1993. A rapid CTAB DNA isolation technique useful for RAPD fingerprinting and other PCR applications. Biotechniques 14, 748–750. https://pubmed.ncbi.nlm.nih.gov/8512694/.

Steyn, E., 1974. Leaf anatomy of *Greyia* Hooker & Harvey (Greyiaceae). Botan. J. Linnean Soc. 69, 45–51. https://doi.org/10.1111/j.1095-8339.1974.tb01613.x.

Steyn, E.M.A., Smith, G.F., Condy, G., 1999. *Greyia flanaganii*. Flowering Plants of Africa 56, 86-92.

Štorchová, H., Olson, M.S., 2007. The architecture of the chloroplast *psbA-trnH* non-coding region in angiosperms. Plant Syst. Evol. 268, 235–256. https://link.springer.com/article/10.1007/s00606-007-0582-6.

Sytsma, K.J., Spalink, D., Berger, B., 2014. Calibrated chronograms, fossils, outgroup relationships, and root priors: re-examining the historical biogeography of Geraniales. Biol. J. Linnean Soc. 113, 29–49. https://onlinelibrary.wiley.com/doi/abs/10.1111/bij.12297.

Szyszyłowicz, I., 1888. *Greyia radlkoferi* Szyszl., Polypetalae disciflorae Rehmannianae, Vol. 2. typis Universitatis Jagellonicae, Cracoviae, pp. 49-50. https://www.biodiversitylibrary.org/item/221296.

Taberlet, P., Gielly, L., Pautou, G., Bouvet, J., 1991. Universal primers for amplification of three non-coding regions of chloroplast DNA. Plant Mol. Biol. 17, 1105–1109. https://doi.org/10.1007/BF00037152.

The Angiosperm Phylogeny Group, 2016. An update of the Angiosperm Phylogeny Group classification for the orders and families of flowering plants: APG IV. Botan. J. Linnean Soc. 181, 1–20. https://doi.org/10.1111/boj.12385.

Van Wyk, B., Van Wyk, P., 2013. Field Guide to Trees of Southern Africa. Struik Nature South Africa. https://books.google.co.za/books?id=dw1bDwAAQBAJ.

Viljoen, E., Odeny, D.A., Coetzee, M.P.A., Berger, D.K., Rees, D.J.G., 2018. Application of Chloroplast Phylogenomics to Resolve Species Relationships Within the Plant Genus Amaranthus. J. Mol. Evol. 86, 216–239. https://doi.org/10.1007/s00239-018-9837-9.

Whitley, B.S., Li, Z., Jones, L., de Vere, N., 2024. Mega-Barcoding Projects: Delivering National DNA Barcoding Initiatives for Plants. In: DeSalle, R. (Ed.), DNA Barcoding: Methods and Protocols. Springer US, New York, NY, pp. 445–473. https://doi.org/10.1007/978-1-0716-3581-0_27.

Wickham, H., 2016. ggplot2: Elegant Graphics for Data Analysis. Springer, Cham. https://doi.org/10.1007/978-3-319-24277-4, 2 ed.

Xu, B., Zeng, X.-M., Gao, X.-F., Jin, D.-P., Zhang, L.-B., 2017. ITS non-concerted evolution and rampant hybridization in the legume genus *Lespedeza* (Fabaceae). Sci. Rep. 7, 40057. https://doi.org/10.1038/srep40057.

Zuntini, A.R., Carruthers, T., Maurin, O., Bailey, P.C., Leempoel, K., Brewer, G.E., Epitawalage, N., Françoso, E., Gallego-Paramo, B., McGinnie, C., Negrão, R., Roy, S. R., Simpson, L., Toledo Romero, E., Barber, V.M.A., Botigué, L., Clarkson, J.J., Cowan, R.S., Dodsworth, S., Johnson, M.G., Kim, J.T., Pokorny, L., Wickett, N.J., Antar, G.M., DeBolt, L., Gutierrez, K., Hendriks, K.P., Hoewener, A., Hu, A.-Q., Joyce, E.M., Kikuchi, I.A.B.S., Larridon, I., Larson, D.A., de Lírio, E.J., Liu, J.-X., Malakasi, P., Przelomska, N.A.S., Shah, T., Viruel, J., Allnutt, T.R., Ameka, G.K., Andrew, R.L., Appelhans, M.S., Arista, M., Ariza, M.J., Arroyo, J., Arthan, W., Bachelier, J.B., Bailey, C.D., Barnes, H.F., Barrett, M.D., Barrett, R.L., Bayer, R.J., Bayly, M.J., Biffin, E., Biggs, N., Birch, J.L., 2024. Phylogenomics and the rise of the angiosperms. Nature 629, 843–850. https://doi.org/10.1038/s41586-024-07324-0.